Supplementary Information (SI) for Journal of Materials Chemistry A.

Suppporting Information

Light−promoted dual coking−elimination effects enable highly efficient photothermocatalytic dry reforming of methane on Ni/CeO_2-Al_2O_3

Jia Guo, Lei Ji, Yuanzhi Li, and Yulu Zhang.*

State Key Laboratory of Silicate Materials for Architectures (Wuhan University of Technology), 122 Luoshi Road, Wuhan 430070, P.R. China.

*Corresponding author.

E-mail address: liyuanzhi@whut.edu.cn

Jia Guo and Lei Ji contributed equally to the paper.

Contents

1. Characterization.

X-ray diffraction (XRD) patterns of the sample were acquired on a RigakuDmax X-ray diffractometer equipped with Cu Kα radiation. Transmission electron microscopy (TEM) images were recorded by a JEM−2100F machine. The composition of the samples was determined on an inductively coupled plasma/optical emission spectroscopy (ICP−OES, Optima 4300DV, PerkinElmer). Nitrogen physisorption measurements were conducted at −196 °C on an ASAP 2020 analyzer to determine the specific surface area and pore size distribution. Thermogravimetric/mass spectrometry (TG−MS) characterization was carried out by the STA449F3 thermal analyzer combined with a mass spectrometer. The Raman spectra were obtained on the LABRAN HR Evolution with excitation of the light source at 532 nm. Diffuse reflectance absorption spectra wereacquired using a UV3600 spectrophotometer. Fourier transform infrared spectra (FTIR) were recorded on an infrared spectrometer (Nicolet 6700).

2. Photothermocatalytic test.

The experimental procedure for the photothermocatalytic dry reforming of methane (DRM) was as follows: a home-made stainless-steel reactor equipped with a quartz window was used. 0.009 g of the sample to be tested was weighed, placed inside, and sealed. A mixture of gases with a composition of 29.6/29.8/40.6 vol% $CH_4/CO_2/Ar$ was continuously introduced into the reactor. The gas flow rate was controlled using a mass flow meter and accurately measured using a soap bubble meter (S49-31/MT). The mixed gas was introduced at a flow rate of 90.50 mL min^{-1} into the reactor. A 500 W Xe lamp with emission across the whole solar spectra (200−2400 nm) was focused on the sample and turned on. The concentrations of reactants and products were analyzed using a GC-9560 gas chromatograph (GC) to evaluate the performance of the sample in the light-driven photothermocatalytic DRM. To investigate the influence of light wavelength on the light-driven photothermocatalytic DRM over the sample Ni/CeO_2-Al_2O_3, long-wave filters with cutoff wavelengths of $\lambda > 420$, 560 or 690 nm were placed in front of the quartz window of the reactor during focused illumination. The power of the focused ultraviolet-visible-infrared (UV−vis−IR) illumination was 6154 mW, and the spot size on the sample, adjusted by a convex lens on the Xe lamp, was approximately 10 mm in diameter. Consequently, the intensity of the focused UV−vis−IR illumination was calculated to be 78.4 kW m^{-2}

(corresponding to a solar flux concentration ratio of 78.4). The power values for the focused visible-infrared (vis−IR) illumination with λ > 420, 560 and 690 nm were 5164, 4476, and 3555 mW, respectively. The concentrations of reactants and products were analyzed using a GC. The methodologies for light-driven photothermocatalytic DRM testing, the quantification of focused illumination power, the determination of sample surface temperatures under concentrated irradiation, the computation of light-to-fuel efficiency, and the gas chromatographic analysis have been comprehensively described in our prior publications.

3. Isotope labeling.

Isotope labeling experiments on Ni/CeO_2-Al_2O_3 samples were carried out using a home-made stainless-steel reactor under UV−vis−IR spotlight illumination. The reactor was connected to the tubular FTIR unit in the room of the infrared spectrometer (Nicolet 6700) through a micropump. 0.009 g of the reduced Ni/CeO_2-Al_2O_3 sample was added to the reactor and the temperature was measured by a thermocouple in close contact with the sample. The gas line was purged with high-purity Ar (60 mL min^{-1}, purified by a deoxygenation tube) for 30 min. After purging, the sample was reduced in a gas stream of 5 vol% H_2, 95 vol% Ar (60 mL min^{-1}, purified by a deoxygenation tube) under UV−vis−IR spotlight for 30 min. After cooling to 400 °C, the flow was switched to a flow of high purity Ar (60 mL min^{-1}, purified by a tube of deoxidant) for removing H_2 adsorbed on the sample for 1 h at 400 °C. Once the pre-reduced sample was cooled to room temperature, the high-purity argon flow was halted, activating the mini-pump, and a gas mixture containing 10 mL of $^{12}C^{18}O_2$, 20 mL of CH_4, and 270 mL of Ar was introduced into the recirculating closed gas line, keeping the mixture to circulate through the system. The Ni/CeO_2-Al_2O_3 was continuously reacted under focused UV−vis−IR illumination, and the data was recorded by using the FTIR spectrometer. At the end of the experiment, keeping the original state unchanged. Once the chamber temperature has dropped to room temperature, perform a 60 min high-purity Ar purge. The sample was subjected to photothermal catalytic DRM experiments in the same way as described above, with the only difference that the gas $^{12}C^{18}O_2$ was replaced by $^{12}C^{16}O_2$.

4. Temperature-programmed desorption of CO_2 (CO_2−TPD).

The CO_2−TPD of Ni/CeO_2-Al_2O_3, Ni/Al_2O_3, CeO_2-Al_2O_3 and Al_2O_3 was examined using a multifunctional adsorption instrument (TP-5080) under dark conditions. 0.025 g sample was placed in a quartz tube and heated at a rate of 10 °C min^{-1} to 700 °C in a flow of 5 vol% H_2/Ar (24 mL min^{-1}) connected to a deoxidizer tube, and held at 700 °C for 60 min. After cooling to 400 °C, the gas flow was switched to high-purity He (24 mL min^{-1}, purified through the deoxidizer tube) and maintained at 400 °C for 60 min in to remove adsorbed H_2. When cooled to room temperature, the gas supply was switched to 10 vol% CO_2/He (24 mL min^{-1}) for CO_2 adsorption. The CO_2 adsorption lasted for 30 min, and then switched back to high-purity He purified by the deoxidizer (24 mL min^{-1}). After the baseline stabilized, the pre-adsorbed CO_2 sample was heated to 750 °C at a rate of 10 °C min^{-1}, and the process curve was recorded using the TP-5080.

5. Photocatalytic tests.

The DRM photocatalytic performance of Ni/CeO_2-Al_2O_3 samples was tested using a homemade stainless-steel reactor at near room temperature. 0.009 g of Ni/CeO_2-Al_2O_3 was taken into the reactor, which was placed in an ice-water bath to ensure that it was close to room temperature under Xe lamp irradiation, and the other steps were the same as those for the measurement of photothermal catalytic activity.

6. Controlled catalytic tests.

DRM on Ni/CeO_2-Al_2O_3 was conducted at various temperatures in the dark or focused illumination using a home-made quartz conical reactor. 0.009 g of the catalyst was pre-reduced with a 5 vol% H_2/Ar flow (30 mL min^{-1}) at 500 °C for 30 min. Following pre-reduction, the 5 vol% H_2/Ar flow was switched to a 10/10/80 vol% CH_4/CO_2/Ar mixture, with the flow rate controlled at 90 mL min^{-1}. The gas concentrations of reactants and products at various temperatures were recorded using a GC in the dark, under focused illumination, and light with wavelengths greater than 420 nm and 560 nm.

7. CH_4 temperature programmed oxidation by pre-adsorbed CO_2 (CH_4−TPO−CO_2).

CH_4 temperature-programmed oxidation by pre-adsorbed CO_2 (CH_4−TPO−CO_2) on the samples of Ni/Al_2O_3 or Ni/CeO_2-Al_2O_3 was conducted in the dark or under focused UV−vis−IR illumination using a home-made quartz conical reactor equipped with a heating device in a circulating air circuit. 0.009 g of the Ni/Al_2O_3 or Ni/CeO_2-Al_2O_3 sample was heated to 500 °C at a rate of 10 °C min^{-1} and maintained at this temperature for 30 min in a reducing atmosphere of 5 vol% H_2/Ar (50 mL min^{-1}), which had been purified using a deoxidizing tube. After cooling to 400 °C, the 5 vol% H_2/Ar flow was replaced with a flow of high-purity argon (50 mL min^{-1}, also purified by a deoxidizing tube) to remove adsorbed hydrogen from the sample for 60 min at 400 °C. Once cooled to room temperature, the argon flow was switched to a flow of pure CO_2 (50 mL min^{-1}) for 30 min to facilitate CO_2 adsorption. Subsequently, the CO_2 stream was replaced with a flow of high-purity argon (50 mL min^{-1}, purified by a deoxidizing tube) to remove any free and physically adsorbed CO_2. Finally, the samples, which had been pre-absorbed with CO_2, were subjected to reaction in the dark or under UV−vis−IR illumination within a circulating gas stream of a CH_4 mixture (20 mL CH_4 mixed with 280 mL of argon, purified by a deoxidizing tube) at a heating rate of 10 °C min^{-1}. The FTIR spectra of the gas composition within the system were recorded throughout the process. After the CH_4−TPO−CO_2 experiments, the used samples were mixed with KBr powder (1:40), pressed into a translucent state, and infrared light was allowed to pass through the samples, and then record the attenuated total reflectance (ATR) spectra of the sample.

8. H_2−TPR of pre-chemisorbed O_2 (H_2−TPR−O_2).

H_2−TPR−O_2 was using a quartz tube reactor which a quartz window attached its bottom and connecting with the TP-5080. 0.008g catalyst was put into the quartz was heated to 500 °C at a rate of 10 °C min^{-1} with a 24 mL min^{-1} 5 vol% H_2/Ar flow and held at 500 °C for 1 h. Then, the temperature was lowered to 400 °C, and high-purity He was blown for 1 h to remove the adsorbed H_2. After cooling to room temperature, the gas was switched to 5 vol% O_2/He with a flow rate of 24 mL min^{-1} and kept 30 min. Pre-treatment completed, the gas was switched to 5 vol% H_2/Ar with a flow rate of 24 mL min^{-1}. Once the airflow is stable, start the TPR program with paralleled UV−vis−IR illumination or in the dark.

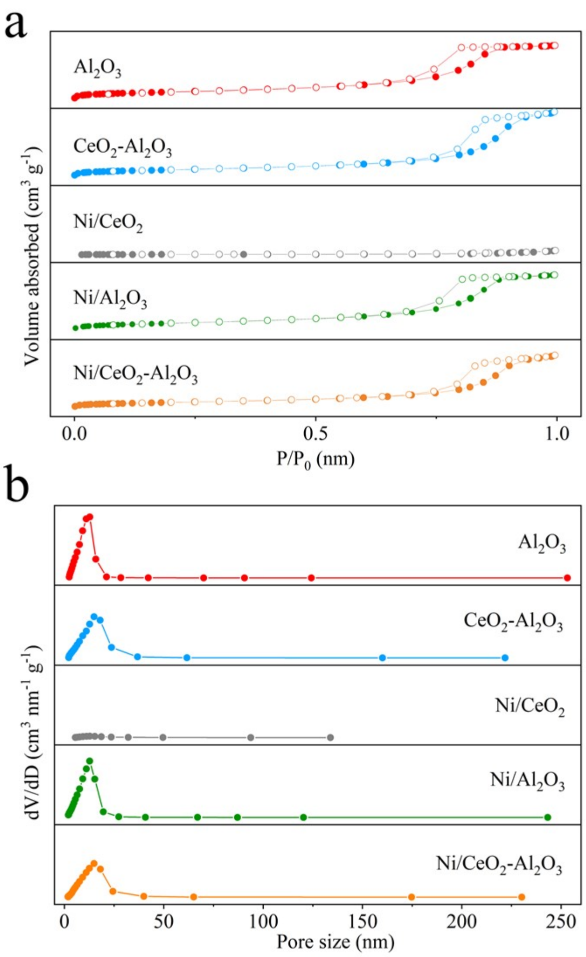

Fig. S1 The N_2 adsorption-desorption isotherms (a) and BJH adsorption pore size distributions (b) for Ni/CeO_2-Al_2O_3, Ni/Al_2O_3, Ni/CeO_2, CeO_2-Al_2O_3 and Al_2O_3.

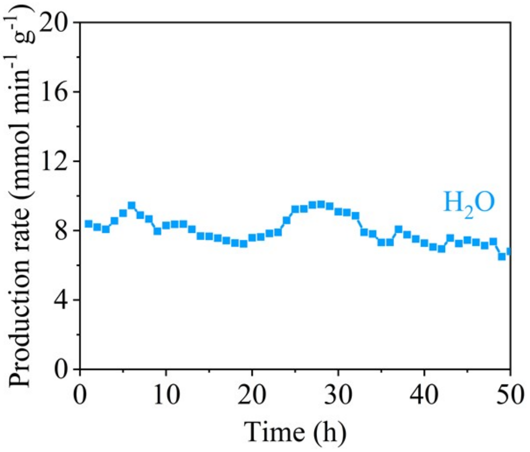

Fig. S2 Time-dependent curves of r_{H2O} during photothermocatalytic DRM on Ni/CeO_2-Al_2O_3.

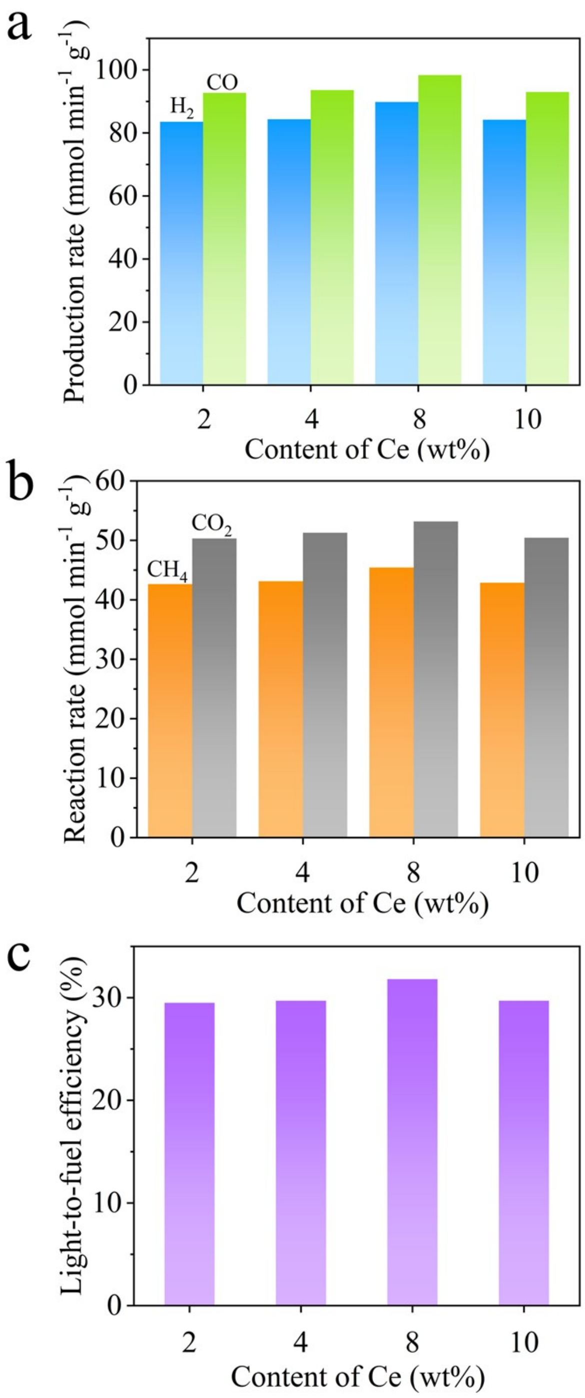

Fig. S3 (a) The production rate of H_2 and CO, (b) the reaction rate of CH_4 and CO_2, and (c) light-to-fuel efficiency of Ni/CeO_2-Al_2O_3 with different Ce contents under concentrated UV−vis−IR illumination.

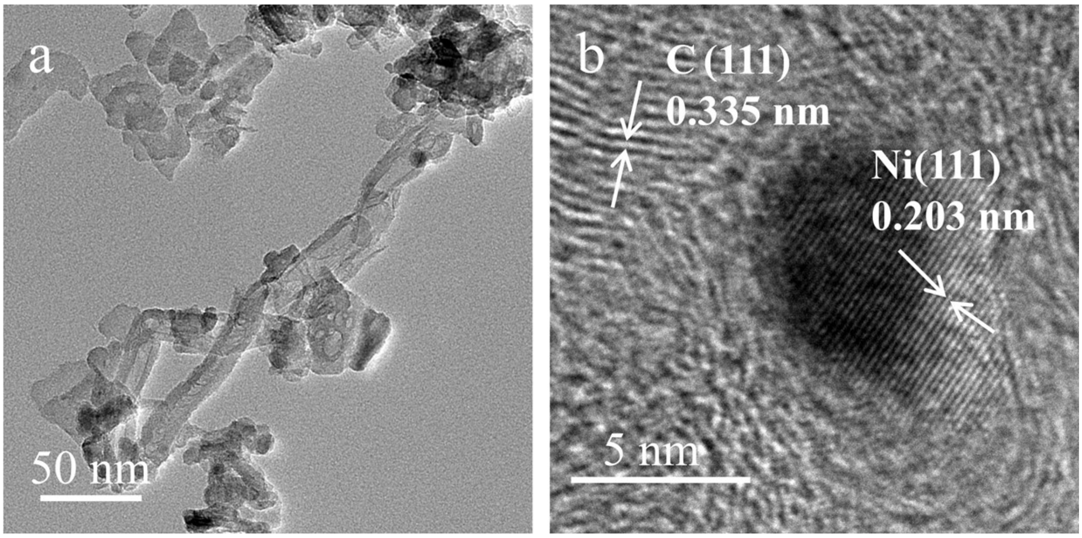

Fig. S4 TEM (A) and HRTEM (B) images of the used Ni/CeO_2-Al_2O_3.

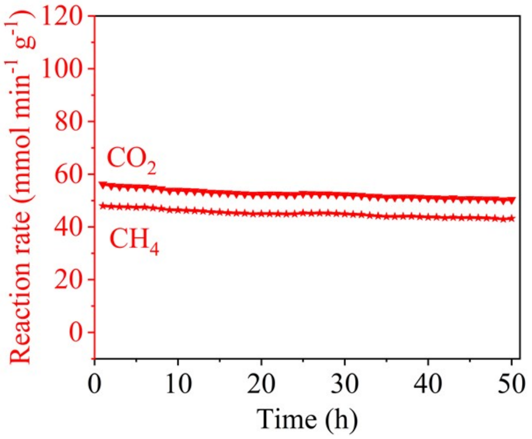

Fig. S5 Time-dependent curves of r_{CO2} and r_{CH4} during photothermocatalytic DRM on Ni/CeO_2-Al_2O_3.

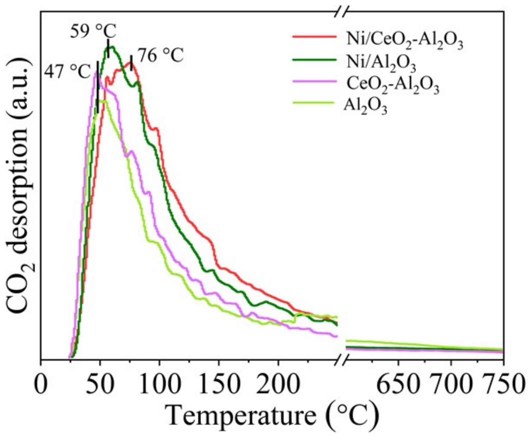

Fig. S6 CO_2−TPD profiles of Ni/CeO_2-Al_2O_3, Ni/Al_2O_3, CeO_2-Al_2O_3 and Al_2O_3 in the dark.

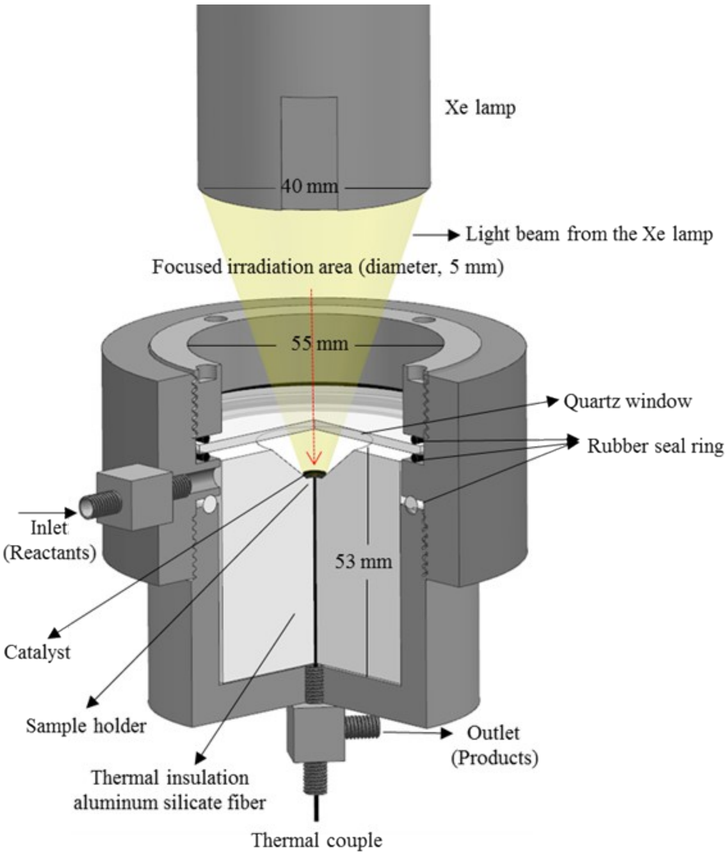

Scheme S1 Schematic illustration of a home-made reactor for conducting photothermocatalytic CO_2 reduction by CH_4 on the samples under focused illumination from a 500 W Xe lamp without using additional electric heater.

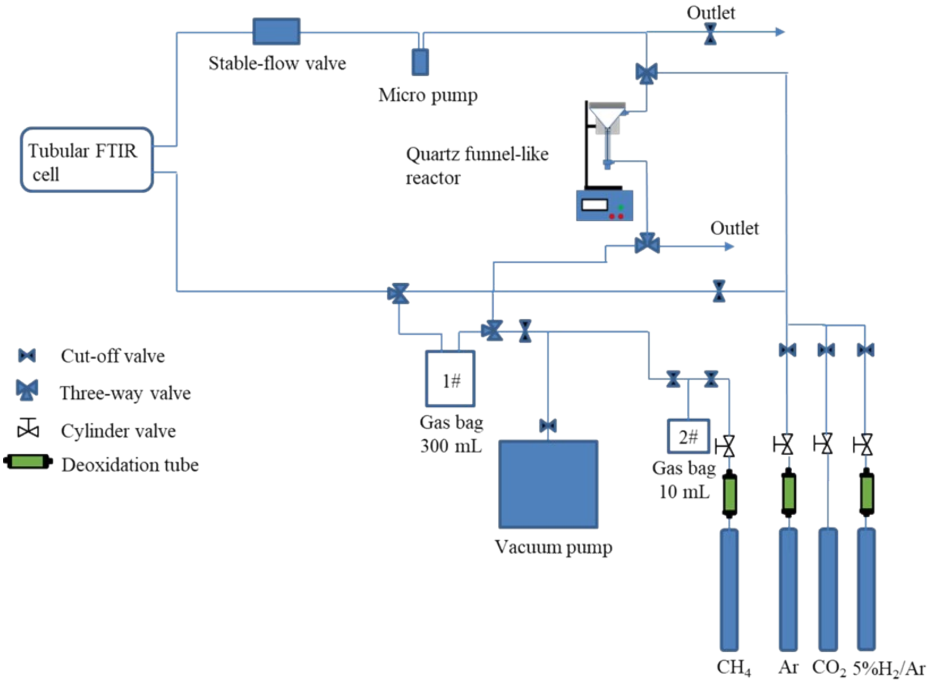

Scheme S2 Set-up for temperature programmed CO_2 desorption and temperature programmed CH_4 oxidation by pre-adsorbed CO_2.

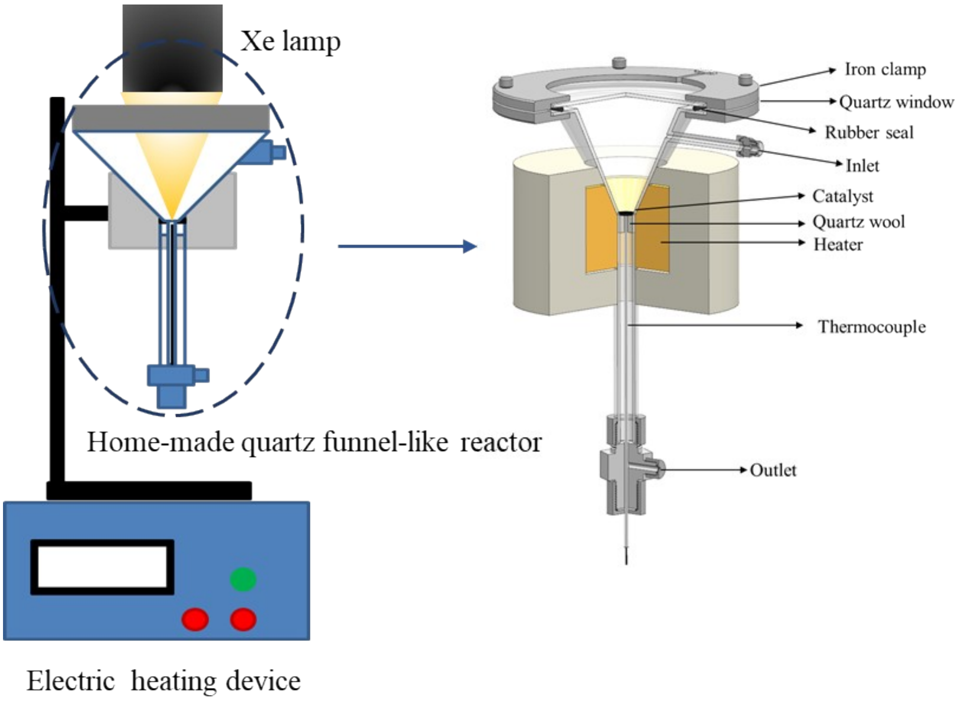

Scheme S3 Schematic diagram of home-made quartz cylindro-conical reactor used in test of CH_4 temperature programmed oxidation by pre-adsorbed CO_2 in the dark and with concentrated UV−vis−IR illumination.

Table S1 The texture structure of catalysts.

sample	Ni (wt%)	Ce (wt%)	Ni crystal size (nm)	CeO_2 crystal size (nm)	BET surface area (m^2 g^{-1})	BJH absorption volume (cm^3 g^{-1})
Ni/CeO_2-Al_2O_3	4.77	6.11	6.8	8.0	94.6	0.36
Ni/Al_2O_3	4.86	0.00	6.2		127.7	0.39
Ni/CeO_2	4.90	77.41	17.8	25.7	5.1	0.03
CeO_2-Al_2O_3				8.3	117.6	0.45
Al_2O_3					129.1	0.38

Table S2 Comparison of photothermocatalytic DRM activity of various catalysts.

Catalyst	Feed composition	Light intensity (kW m^{-2})	H_2 production rate (mmol g^{-1} min^{-1})	Light-to-fuel efficiency (%)	Coke deposition rates ($g_C \cdot g^{-1}_{catalyst} \cdot h^{-1}$)	Reference
Ni/CeO_2-Al_2O_3	30/30/40 vol% CH_4/CO_2/Ar	78.4	94.61	33.5	1.75× 10^{-3}	This work
Ni-CeO_2/SiO_2	29.5/30/40.5 vol% CH_4/CO_2/Ar	385.2	33.42	27.4	1.25× 10^{-2}	56
Ni/CeO_2	9.8/10/80.2 vol% CH_4/CO_2/Ar	363.4	6.53	11.0	1.25× 10^{-2}	63
Ni-La_2O_3/SiO_2	19.9/20/60.1 vol% CH_4/CO_2/Ar	410.9	38.11	20.3	3.75× 10^{-3}	42
Pt/CeO_2-MNR	10.2/10.2/79.6 vol% CH_4/CO_2/Ar	371.1	5.70	10.6		33
Ru/CeO_2	28.5/29.7/41.8 vol% CH_4/CO_2/Ar	354.2	57.37	26.6	5.26× 10^{-5}	32
SCM-Ni/SiO_2	11.7/11.5/76.8 vol% CH_4/CO_2/Ar	343.6	17.10	12.5	3.93 × 10^{-6}	39
Ni/Ni-Al_2O_3	19.4/19.3/61.3 vol% CH_4/CO_2/Ar	333.8	27.02	19.9	1.70× 10^{-2}	38
5% Ni AMOMs EG	48/48/4 vol% CH_4/CO_2/Ar	37	38.57	24.0		19